AD-781 592

CONTINUED DEVELOPMENT-TWO STAGE HIGH-PRESSURE-RATIO CENTRIFUGAL COMPRESSOR

Colin Rodgers

Solar

EUSTIS DIRECTORATE POSITION STATEMENT

This contractual effort is a continuation of work performed under the terms of Contract DAAJ02-72-C-0014, wherein the contractor demonstrated the basic performance potential of a two-stage centrifugal compressor but with limitations in speed due to a first-stage shroud distortion problem.

The full performance predicted for the two-stage compressor on the basis of individual stage tests was not realized; however, the actual performance achieved is considered to substantiate an impressive alternative to other compressor configurations for small gas turbine engines. There were no problems identified that detract from expectations of achieving the design performance with further development.

This report has been reviewed by technical personnel of this directorate. The conclusions contained herein are concurred in by this directorate and will be considered in any future centrifugal compressor programs.

The U.S. Army project engineer for this effort was Mr. R. A. Langworthy, Technology Applications Division.

AD-781592

SECURITY CLASSIFICATION OF THIS PAGE (When Data Entered)

REPORT DOCUMENTATION PAGE		READ INSTRUCTIONS BEFORE COMPLETING FORM
1. REPORT NUMBER USAAMRDL-TR-74-20	2. GOVT ACCESSION NO.	3. RECIPIENT'S CATALOG NUMBER
4. TITLE (and Subtitle) CONTINUED DEVELOPMENT–TWO-STAGE HIGH-PRESSURE-RATIO CENTRIFUGAL COMPRESSOR		5. TYPE OF REPORT & PERIOD COVERED Final
		6. PERFORMING ORG. REPORT NUMBER ER 2460
7. AUTHOR(s) Colin (NMI) Rodgers		8. CONTRACT OR GRANT NUMBER(s) DAAJ02-73-C-0045
9. PERFORMING ORGANIZATION NAME AND ADDRESS Solar, Division of International Harvester Company 2200 Pacific Highway San Diego, CA 92112		10. PROGRAM ELEMENT, PROJECT, TASK AREA & WORK UNIT NUMBERS Task 1G162207AA7102
11. CONTROLLING OFFICE NAME AND ADDRESS Eustis Directorate U.S. Army Air Mobility R&D Laboratory Fort Eustis, VA 23604		12. REPORT DATE April 1974
		13. NUMBER OF PAGES 41
14. MONITORING AGENCY NAME & ADDRESS(If different from Controlling Office)		15. SECURITY CLASS. (of this report) Unclassified
		15a. DECLASSIFICATION/DOWNGRADING SCHEDULE

16. DISTRIBUTION STATEMENT (of this Report)

Approved for public release; distribution unlimited.

17. DISTRIBUTION STATEMENT (of the abstract entered in Block 20, if different from Report)

D D C
RECEIVED
JUL 11 1974
D

19. KEY WORDS (Continue on reverse side if necessary and identify by block number)

Compressors
Centrifugal Compressors
Gas Turbines

Details of illustrations in
this document may be better
studied on microfiche.

20. ABSTRACT (Continue on reverse side if necessary and identify by block number)

This report presents the results of a continued compressor technology program directed toward development of a small, advanced, two-stage centrifugal compressor designed to attain high pressure ratios with fixed geometry.

Extensive compressor performance data were obtained for two test configurations. The second test configuration, incorporating a minor rematch to the first-stage compressor components, and operating at a design speed of 82,000 rpm, gave a peak adiabatic efficiency of 78 percent with a pressure ratio of 13.2 and a corrected airflow of 1.94 pps.

DD FORM 1473 1 JAN 73   EDITION OF 1 NOV 65 IS OBSOLETE

SECURITY CLASSIFICATION OF THIS PAGE (When Data Entered)

Block 20

The compressor exhibited extremely wide flow ranges between surge and choke, with peak efficiencies away from the surge line.

PREFACE

This technical report covers all experimental work necessary to fulfill the requirements of Contract DAAJ02-73-C-0045, DA Task 1G162207AA7102, with the Eustis Directorate, U.S. Army Air Mobility Research and Development Laboratory, Fort Eustis, Virginia.

The technical representative of the U.S. Army was Mr. R. A. Langworthy of the Eustis Directorate. The principal investigator responsible for the technical content execution and program liaison was C. Rodgers. Other Solar personnel engaged in the program included J. Thayer, Experimental Engineer, M. Lafferty, Design Engineer, and D. Smith, Test Technician.

TABLE OF CONTENTS

Preceding page blank

LIST OF ILLUSTRATIONS

LIST OF ILLUSTRATIONS - Continued

INTRODUCTION

USAAMRDL Technical Report 73-4* contains the results of a compressor technology program directed toward development of a small, two-stage, high-pressure-ratio centrifugal compressor.

Preliminary compressor rig performance data showed improved state-of-the-art efficiencies, pressure ratio capability, and flow ranges. However, mechanical problems were experienced in running at the 100 percent design speed of 82,000 rpm, because of thermal distortion of the compressor casing.

As a result of demonstrated improved performance capabilities, a continuation program was implemented to modify the compressor rig to prevent recurrence of the distortion problem and enable acquisition of design speed data. Two tests were to be conducted: one with design component matching, followed by a retest with a possible diffuser rematch.

The continued compressor test program and test results are described in this report.

---

*TWO-STAGE HIGH-PRESSURE-RATIO CENTRIFUGAL COMPRESSOR, USAAMRDL Technical Report 73-4, Eustis Directorate, U. S. Army Air Mobility Research and Development Laboratory, Fort Eustis, Virginia, March 1973, AD 759499.

DISCUSSION OF WORK PERFORMED

RIG MODIFICATION

During first tests of the Build 1 two-stage compressor rig*, asymmetric thermal distortion of the outer casing scroll was experienced, causing permanent misalignment of the first-stage front shroud. Subsequent stress and deflection calculations made on the casing, using a two-dimensional, finite element program, revealed that the distortion could be significantly reduced by the addition of stiffer longitudinal plate elements or gussets. The scroll casing gussets were therefore reworked as shown on Figure 1.

The first-stage diffuser boundary layer bleed system was also modified to incorporate a single ducted manifold and an on/off control valve, thereby permitting rapid changeover from no-bleed to bleed conditions during test. The manifold and control valve arrangement is also shown on Figure 1. Figure 2 shows the bleed slots in the first-stage diffuser ahead of the throat.

APPARATUS AND PROCEDURES

Testing of the two-stage compressor turbodrive rig was accomplished using the same test cell arrangement, instrumentation, and test procedures as described in TR 73-4. Two basic performance evaluation tests were conducted:

> Build 2　　Design configuration
>
> Build 3/4　Rematched configuration

For Build 3/4 testing, rig instrumentation was extended to include a proximity probe for determination of the axial displacement of the rotating assembly relative to the casing. Mounting of the probe in the inlet duct system is shown on Figure 3. Measurements from the proximity probe, together with impeller flowering data (TR 73-4, Figure 5), were used to assess the reduction in first- and second-stage impeller axial clearance as temperatures (and speed) increased. Due to the unusually large displacement of the rotating assembly relative to the stationary casing (on the order of 0.032 inch at 100 percent speed), it was necessary to reshim the first stage for operation above 90 percent design speed to avoid rubbing contact. Although maximum performance was exhibited on rubbing contact, it was learned from Builds 1 and 2 that it was not possible to maintain the zero-clearance condition, because of the unmatched thermal response rates of the rotor and casing. Furthermore, any practical application of the compressor would probably require finite operating clearances.

The first- and second-stage impeller axial clearances were duly determined from the probe data and are identified on the respective test performance characteristics.

---

*Ibid.

2

Figure 1. Compressor Rig Modifications.

3

Figure 2.   First-Stage Diffuser Bleed Slots.

4

USING THE (3) 0.196 DIA HOLES IN THE
DSK 14215 MOUNT AS A GUIDE, DRILL AND
TAP 112801-70 FOR 10-32 UNF THD THRU.
INSTALL (3) EA 10-32 HEX SOCKET HD
CAP SCREWS AND FILE ENDS FLUSH WITH
BORE OF 112801-70

112801-70

DSK 14216-1

DSK 14216-2, LOCTITE THREADS
AT FINAL ASSEMBLY

(3) EACH 0.08 THICK RADIAL
STRUTS EQUALLY SPACED.
FULL RADIUS ON LEADING
AND TRAILING EDGES.

10-32 HEX SOCKET HD
SETSCREW - TOP OF SCREW
NOT TO PROTRUDE INTO
AIRSTREAM

HAND BLEND EDGE

DSK 14215

DSK 14217

BENTLY NEVADA 306L36
PROXIMITY PROBE.
INSTALL PER TEST
ENGINEER'S INSTRUCTION

DIMENSIONS IN INCHES

Figure 3. Proximity Probe Installation.

Compressor overall and stage performances were calculated as described in TR 73-4 on the basis of a constant specific heat ratio (γ of 1.395). A computation of the potential error, using a constant specific heat analysis compared with a true enthalpy (or variable specific heat) analysis for overall efficiency, was made. The results are shown on Figure 4. At a pressure ratio of 14.0:1, with an inlet temperature near test conditions of 50°F, the difference between constant and variable specific heat overall efficiencies is 1.3 percentage points.

TEST RESULTS

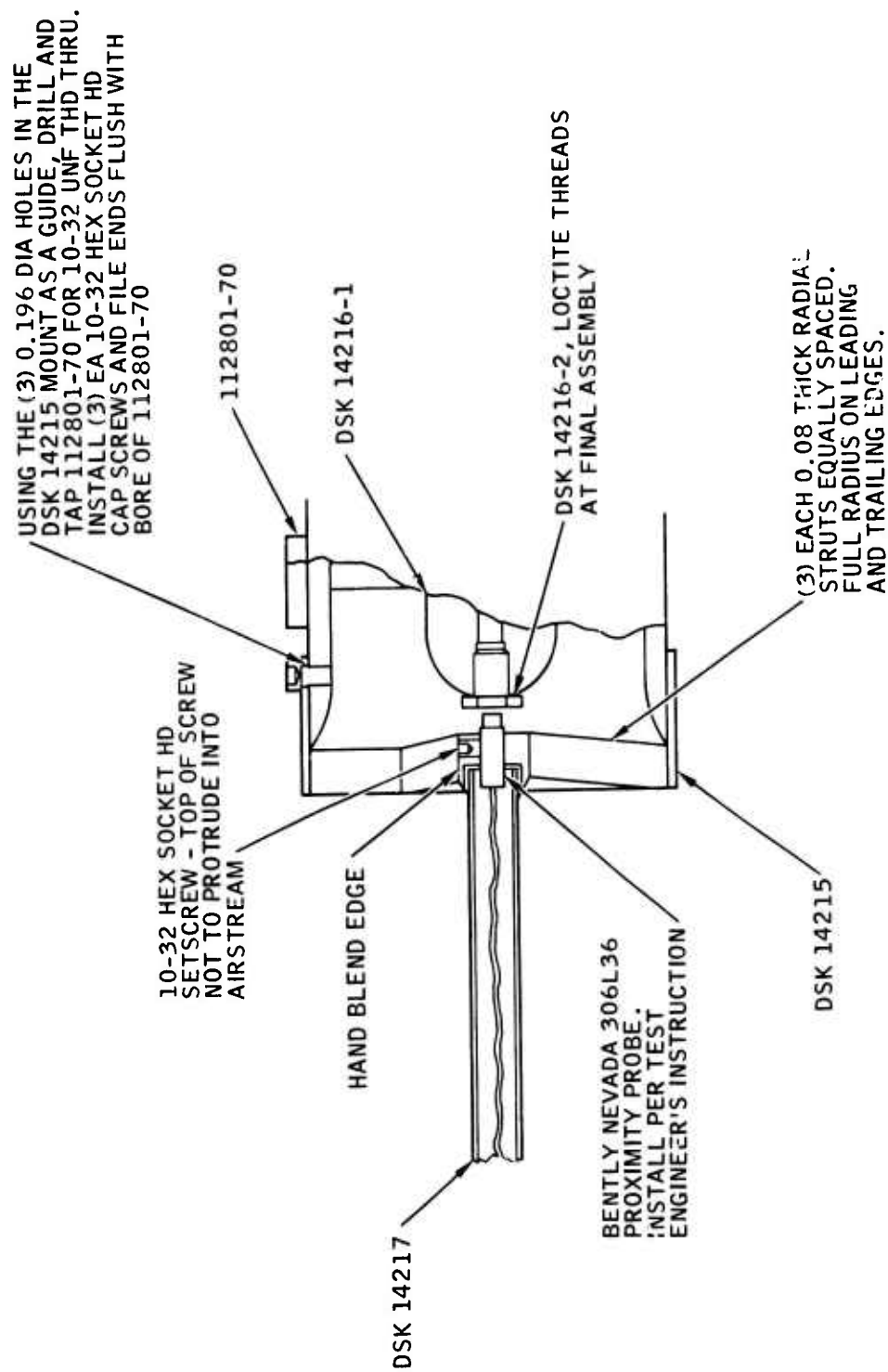The test performance results of the Build 2 and Build 3/4 two-stage centrifugal compressor are presented in the following paragraphs. Note that impeller and diffuser performances were calculated according to the procedure described in TR 73-4, and are presented basically to illustrate relative stage matching and not to indicate absolute impeller efficiency and diffuser recovery levels.

Build 2

The two-stage compressor turbodrive rig, with the casing and bleed manifold modifications incorporated, was assembled for test with first- and second-stage impeller cold axial clearances of 0.016 and 0.015 inch respectively. Calibrations were conducted with zero and 1-1/2 percent first-stage diffuser throat bleed up to 95 percent speed, after which a heavy rub was encountered, requiring a shutdown. Inspection of the first-stage shroud revealed that the first-stage impeller had moved forward into the abradable shroud to increase the cold clearance to 0.044 inch, indicating a possible hot displacement on the order of 0.028 inch.

The abradable shroud rub is shown on Figure 5 and was relatively clean with no pickup on the impeller blades. It was subsequently reasoned that the rub resulted from different thermal response rates of the large mass casing and smaller mass rotating assembly. Operation to higher speeds and temperatures would therefore result in further differential movement of the impeller into the abradable shroud. Installation of a proximity probe to measure the axial displacement was considered, but this would have necessitated a prolonged delay in the test schedule. Accordingly, it was decided to finish the high speed testing with the increased, cold first-stage axial clearance and consider installation of a proximity probe on the next build. Test performance was subsequently obtained at 100 and 103 percent design speed with zero bleed and 100 and 95 percent with 1-1/2 percent diffuser throat bleed. The rig was removed from the test facility and dispatched to the assembly shop for clearance examination. Clearance measurements revealed that the cold first- and second-stage clearances upon termination of Build 2 testing were 0.053 and 0.027 inch respectively. Abrasion of the second-stage shroud had resulted in a near-perfect rubbing condition, as shown on Figure 6. As a consequence of the uniformity, depth, and finish of the rub, it was decided to leave the shroud intact for Build 3 testings. Asymmetric distortion of the casing bore was on the order of 0.004 inch; thus the stiffer casing gussets appeared to have cured the distortion problems experienced on Build 1.

METHOD:

1. $T_2 = T_1 \left[1 + \dfrac{(P_2/P_1)^{\frac{\gamma-1}{\gamma}} - 1}{\eta \text{ Const Prop}} \right]$

2. $\Delta H_{\text{Var Prop}} = \displaystyle\int_{T_1}^{T_2} C_p(T)\,dT$

3. Find T_2' From $P_2/P_1 = e^{\frac{J}{R} \int_{T_1}^{T_2'} \frac{C_p(T)}{T} dt}$

4. $\Delta H' = \displaystyle\int_{T_1}^{T_2'} C_p(T)\,dT$

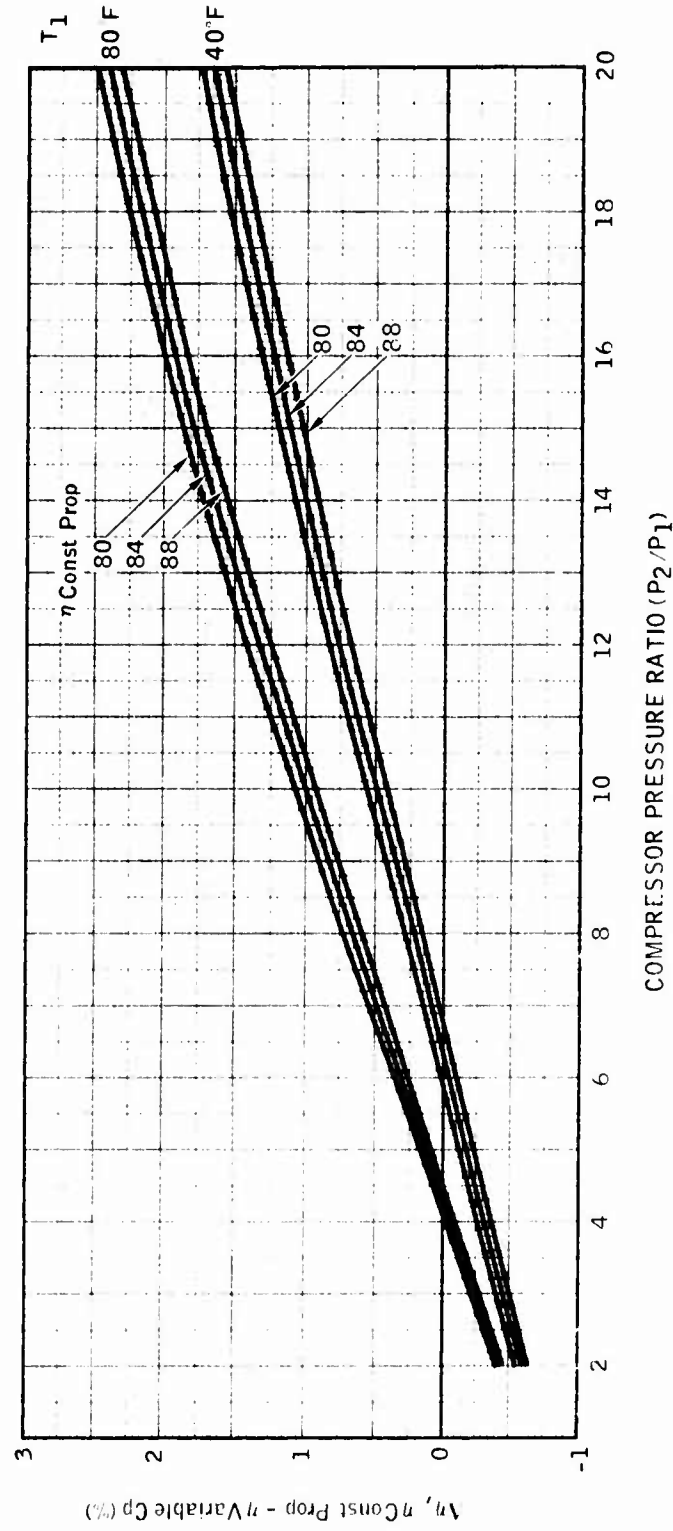5. $\Delta\eta = \eta \text{ Const Prop} - \dfrac{\Delta H'}{\Delta H_{\text{Var Prop}}}$

Figure 4. Difference in Compressor Efficiencies Calculated From Constant and Variable Cp (γ Const. Prop. = 1.3950).

7

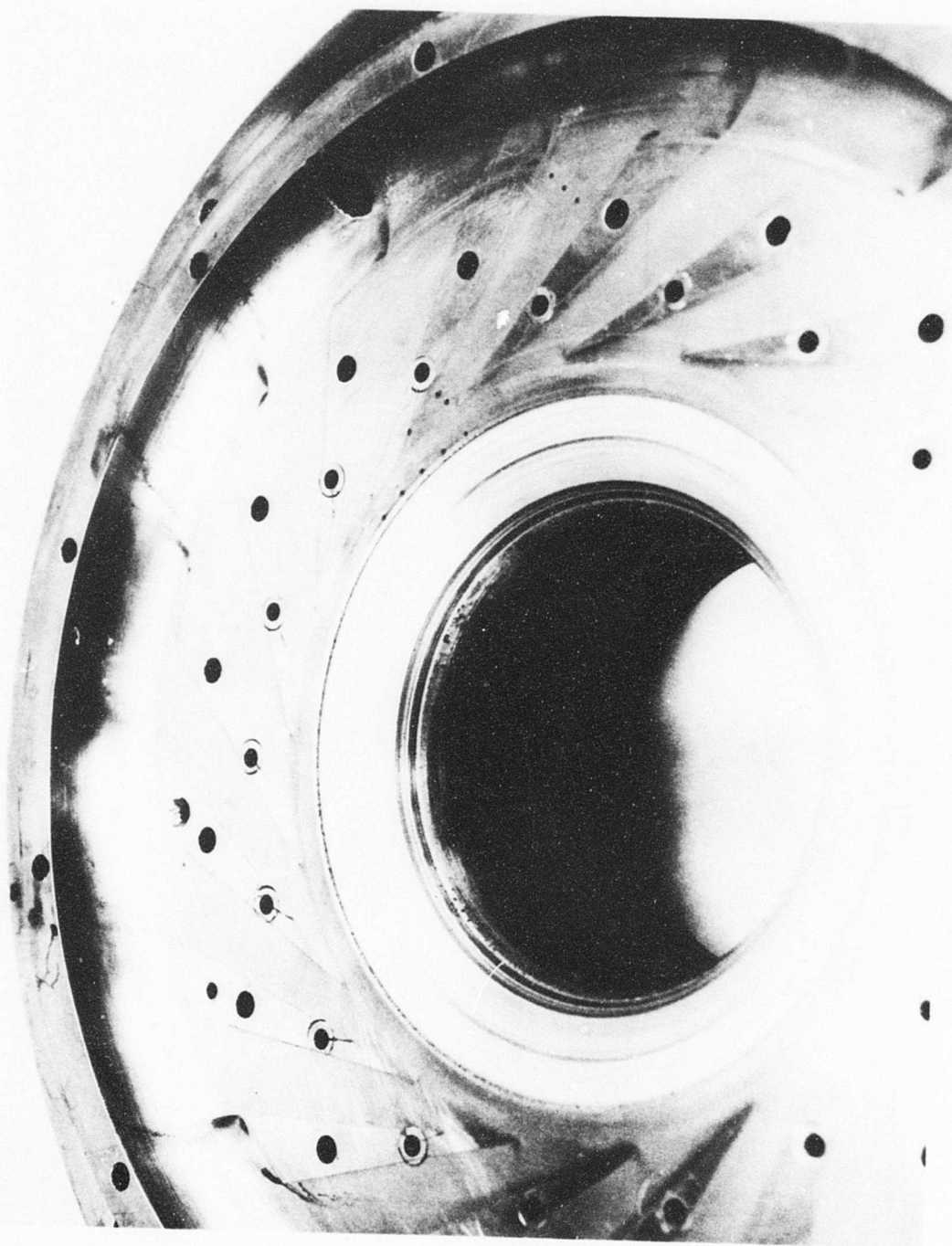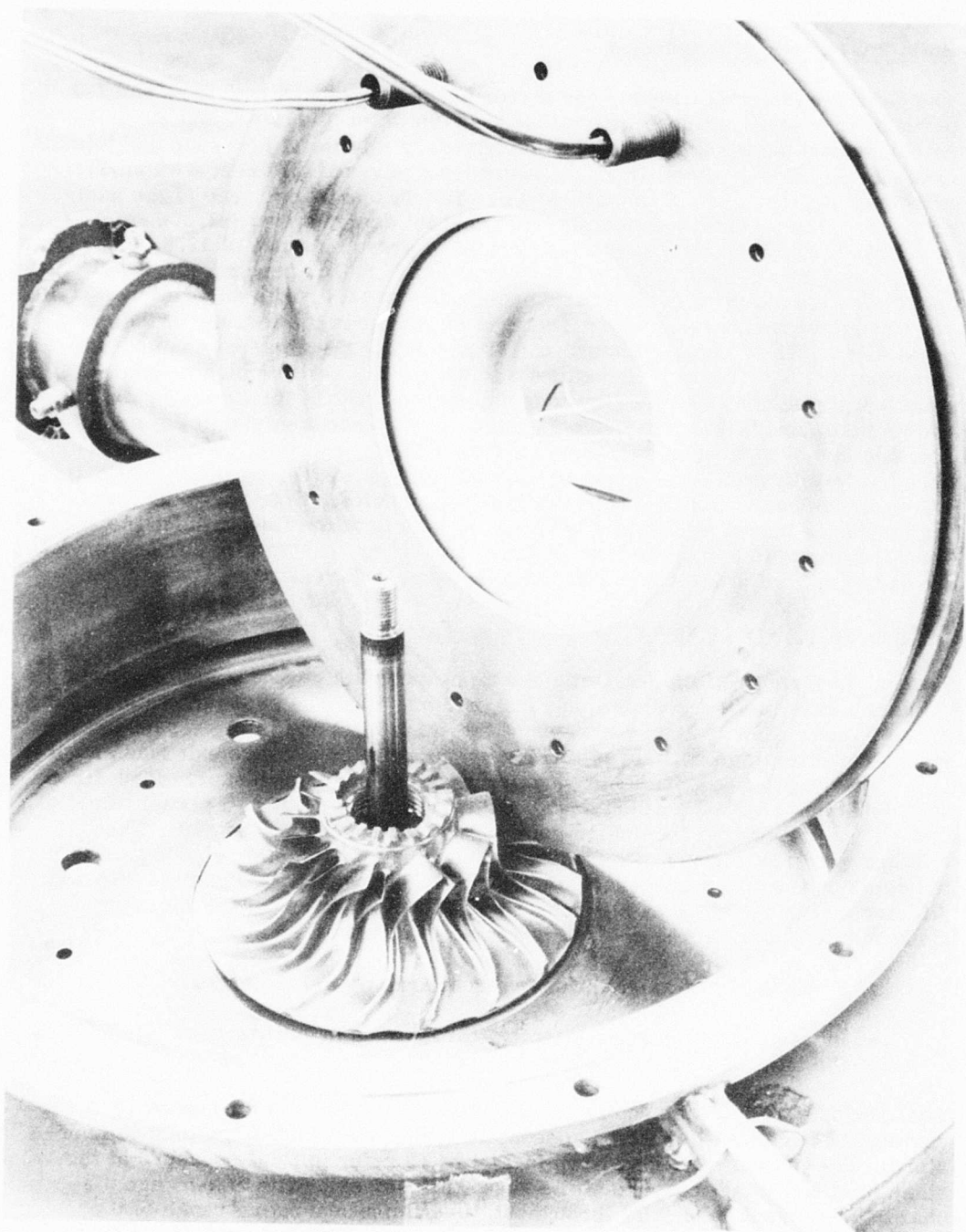Figure 5. First-Stage Shroud Rub.

8

Figure 6.   Second-Stage Shroud Rub.

9

Build 2 Overall Performance

The corrected overall compressor performance, measured with zero and 1-1/2 percent first-stage diffuser throat bleed, is shown on Figures 7 and 8. The performances shown are based upon compressor inlet total pressure and total pressure at the exit scroll from the second-stage vaned diffuser, with an average exit Mach number of 0.17 throughout the efficient operating range of the compressor. Peak overall efficiency at 100 percent design speed (82,000 rpm corrected) with zero bleed was 77 percent at a pressure ratio of 12.6, increasing slightly to 77.5 percent with 1-1/2 bleed takeoff. At 103 percent corrected speed, the maximum pressure ratio recorded was 14.0, with an efficiency of 76.5 percent. The compressor was not surged at 103 percent, because of the close proximity of the overspeed shutdown (108 percent). The general shape of the compressor characteristic and surge line with 1-1/2 percent bleed shows excellent agreement with the previous data from Build 1 (TR 73-4, Figure 19), except that overall peak efficiency is up to 1-1/2 percentage points lower, presumably due to clearance differences. Compressor peak overall efficiencies, based upon inlet-total-to-discharge-scroll static pressure, were approximately 1 percentage point less than total-to-total efficiencies. Note, however, that the discharge scroll was basically designed to collect the flow without any special attempt to complete further diffusion. Thus, essentially no recovery of the dynamic head at the vaned diffuser discharge was realized.

Build 2 Stage Performances

Test performances of the first-stage compressor with zero and 1-1/2 percent diffuser throat bleed are shown on Figures 9 and 10. The pressure ratios shown in the figures refer to total pressure at the stage inlet and total pressure at the exit of the interstage crossover turning vanes, with an average exit Mach number of 0.17 throughout the efficient operating range of the compressor. Peak first-stage efficiency at 100 percent design speed was 77 percent at a pressure ratio of 4.7, compared with the design point values of 81 percent and 4.9. The reduced performance is a consequence of the onset of impeller choking, as indicated by the speed line characteristic at 103 percent speed and the impeller/diffuser matching shown in Figures 11 and 12. As a result of the impeller approaching choke, it was decided to rematch to "unchoke" by:

- Reducing first-stage diffuser throat area by 3-1/2 percent.

- Increasing the inducer effective throat area by cutting back the inducer intermediate short blades.

Test performance of the second-stage compressor is shown on Figure 13 at the various average test-corrected speeds, based upon second-stage inlet temperature. The pressure ratios shown in Figure 13 refer to total pressure at the stage inlet and total pressure at the vaned diffuser exit (with an average discharge Mach number of 0.17 throughout the efficient operating range of the second stage). At 100 percent design speed, peak efficiency was 84 percent (based on $y = 1.395$) with a pressure ratio of 2.7, compared with the design
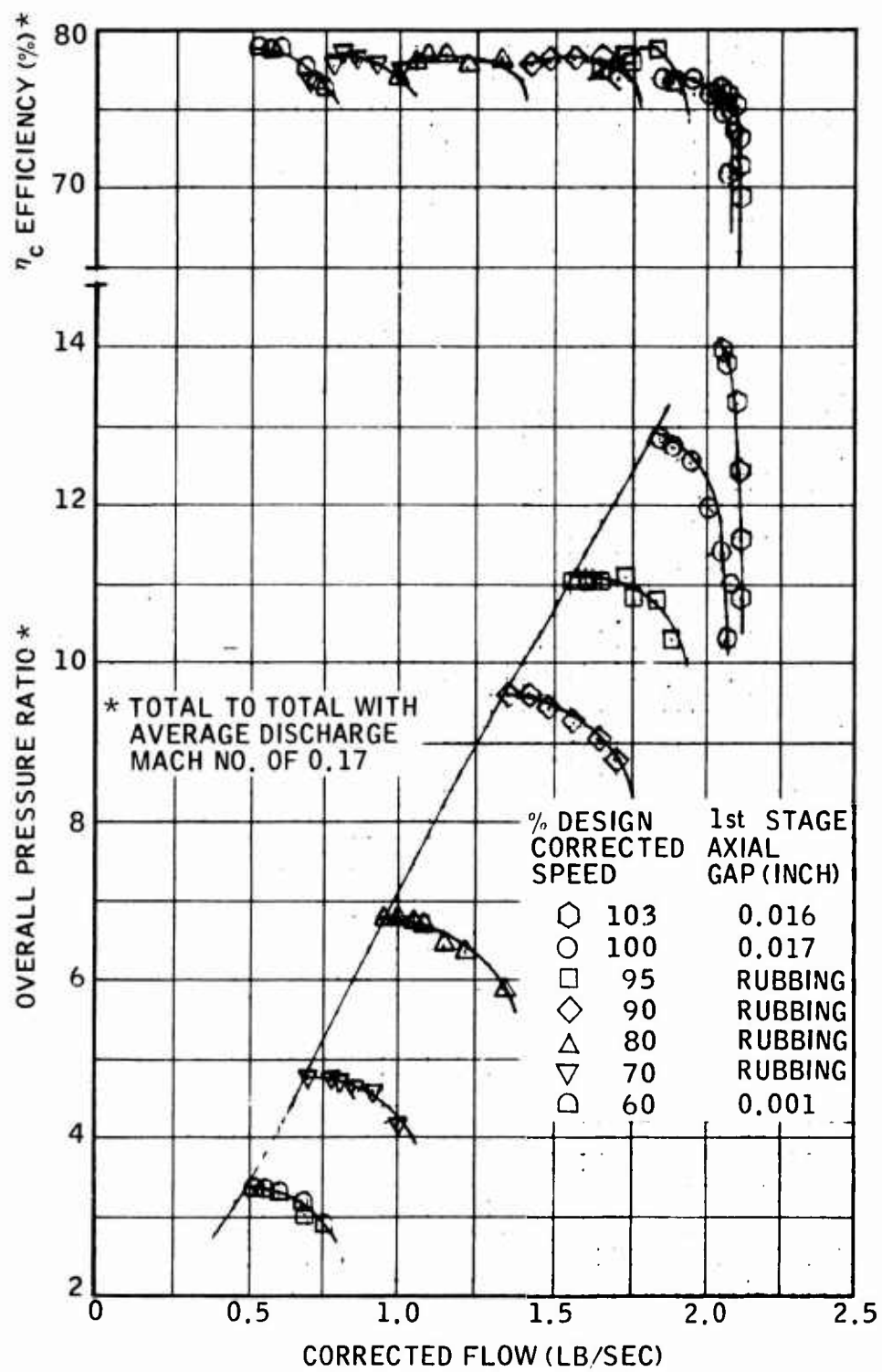
10

Figure 7. Overall Compressor Performance, Build 2 (Zero Bleed).

11

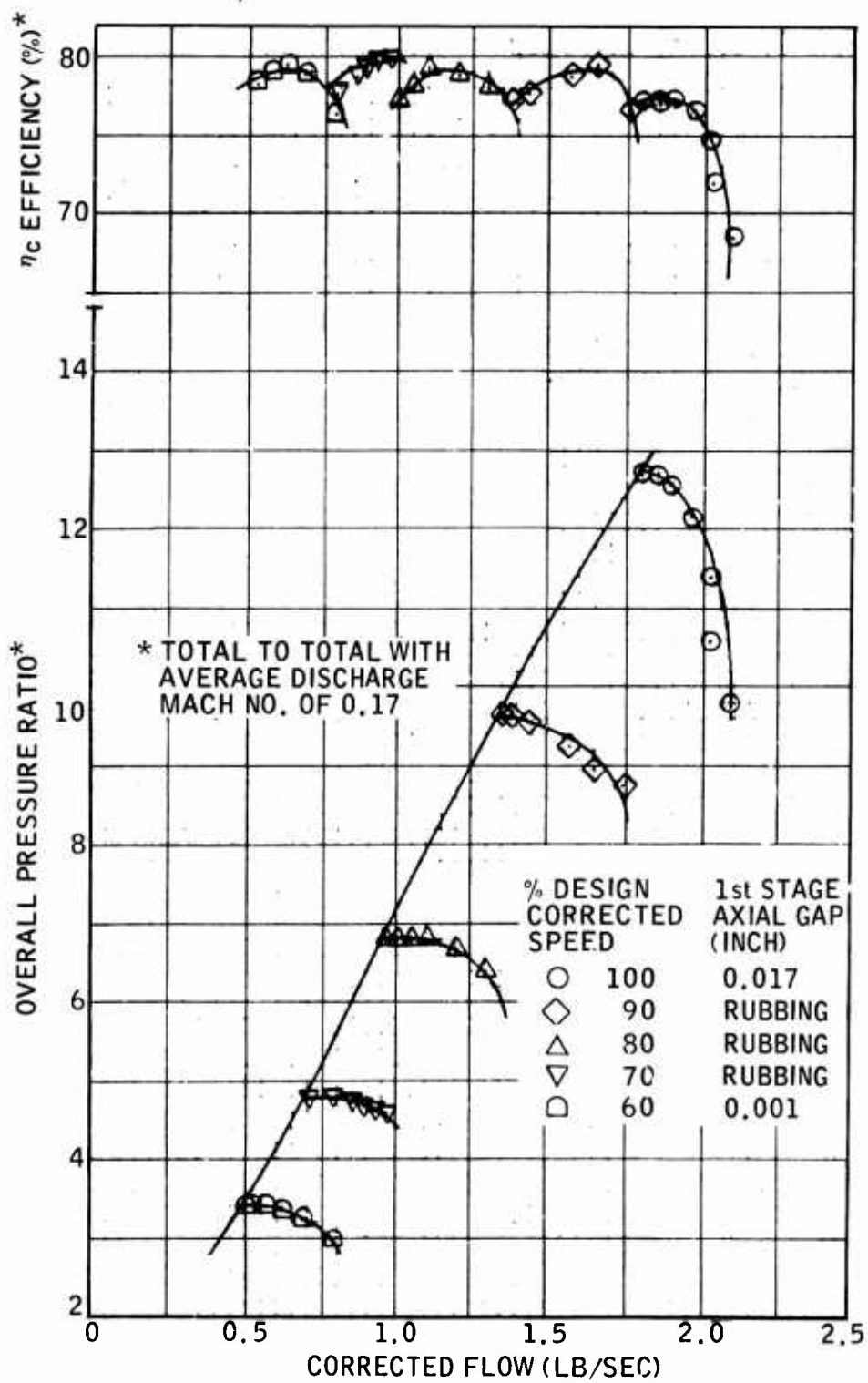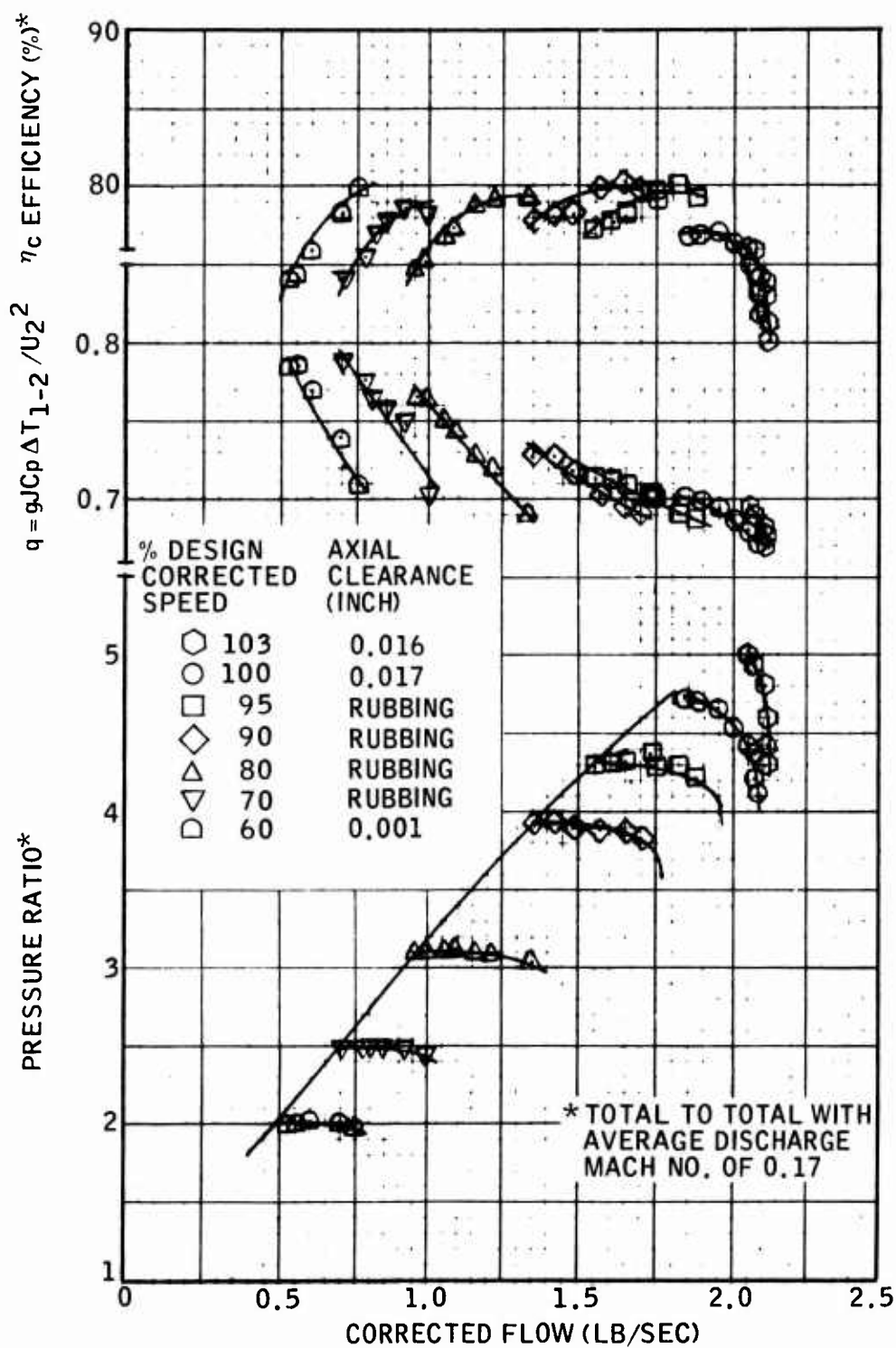Figure 8. Overall Compressor Performance, Build 2 (1-1/2 Percent Bleed).

12

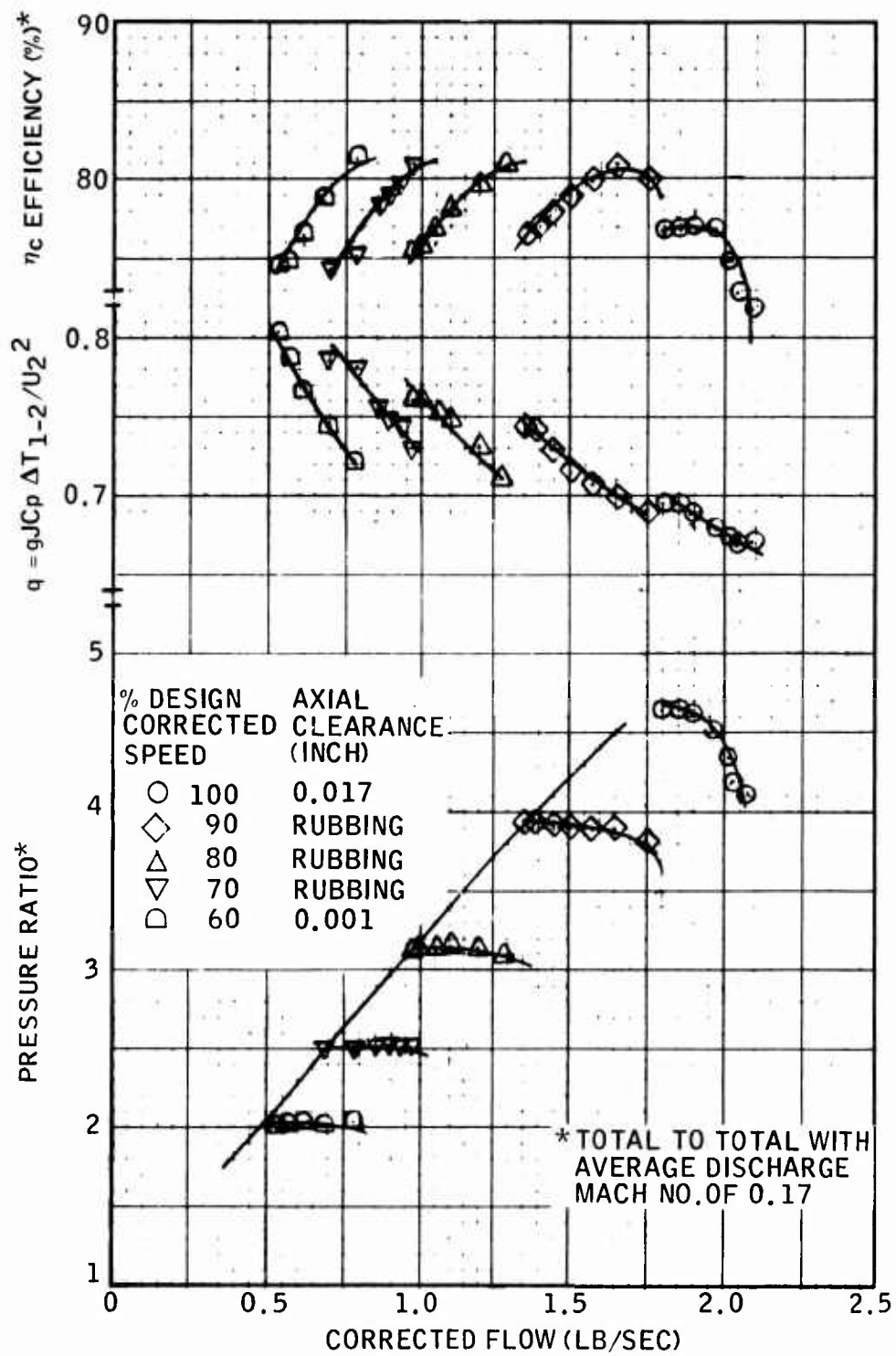Figure 9.   First-Stage Performance, Build 2 (Zero Bleed).

Figure 10.   First-Stage Performance, Build 2 (1-1/2 Percent Bleed).
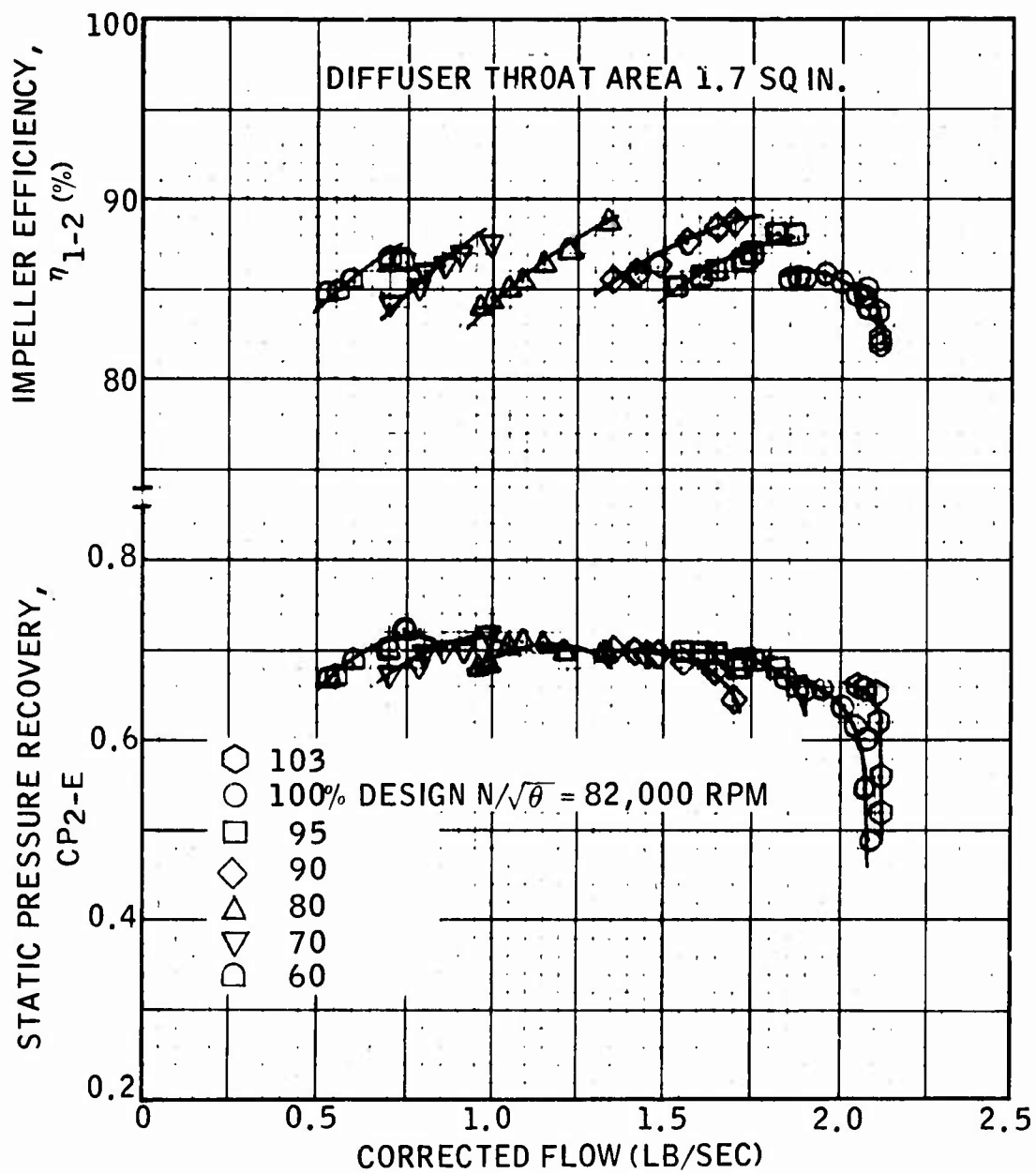
14

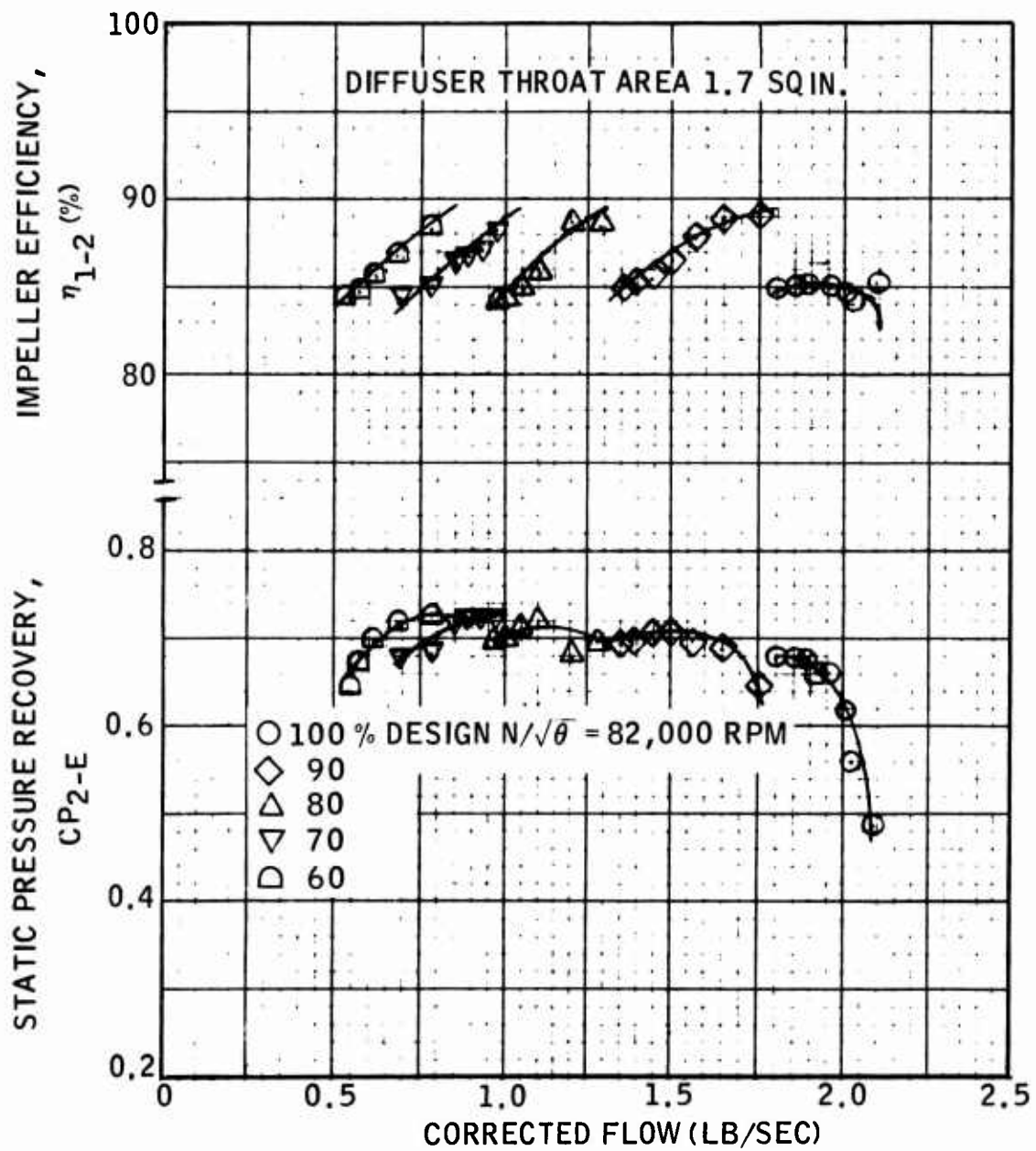Figure 11. First-Stage Impeller and Diffuser Matching, Build 2 (Zero Bleed).

15

Figure 12.   First-Stage Impeller and Diffuser Matching, Build 2
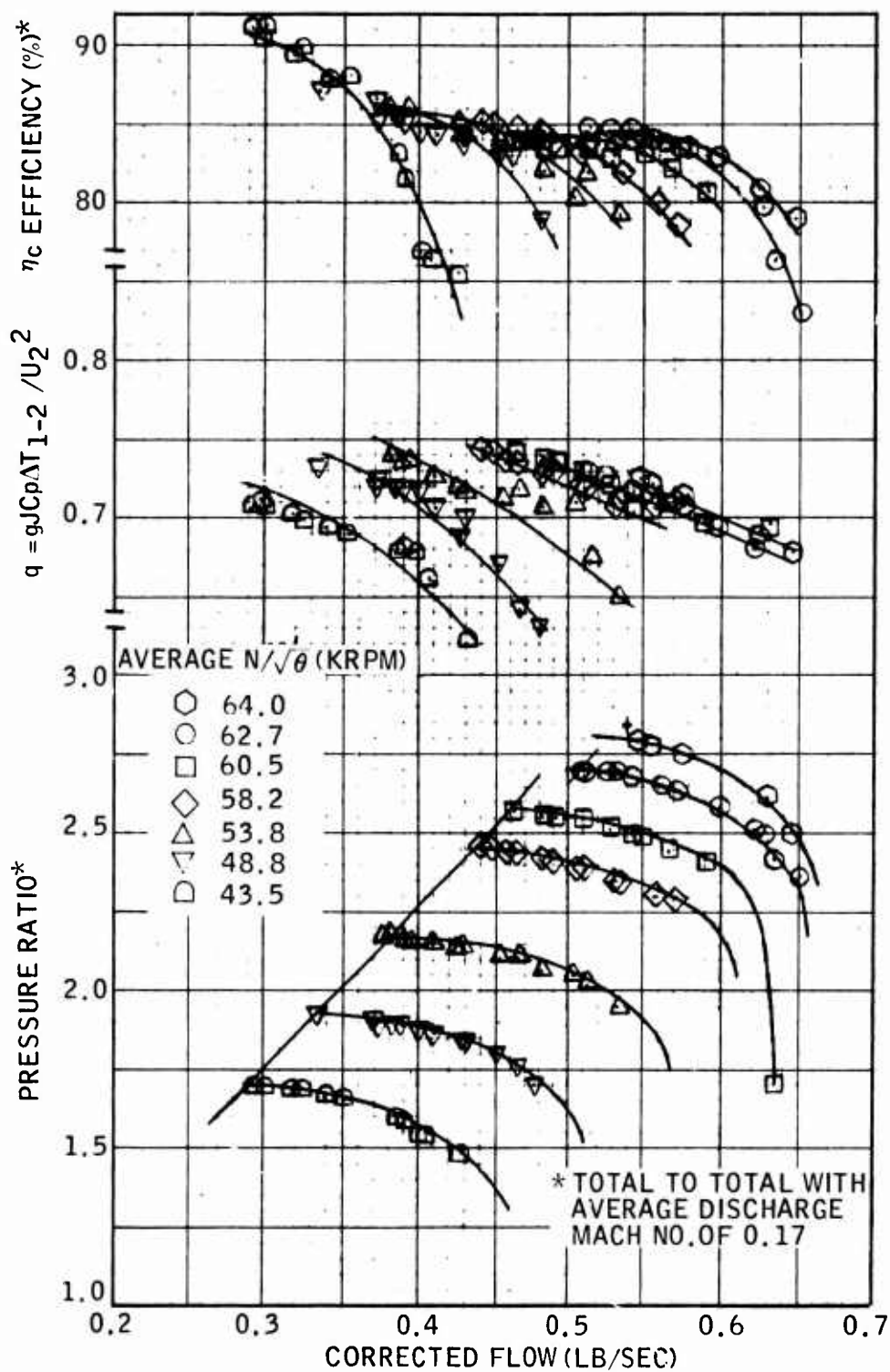(1-1/2 Percent Bleed).

16

Figure 13. Second-Stage Performance, Build 2.

values of 83 percent and 2. 86. Operation to 103 percent design speed increased the pressure ratio to 2.80, with no change in peak efficiency. The relative matching of the second-stage impeller and its vaned diffuser is shown in Figure 14.

Comparison of the efficiency characteristics of the first- and second-stage compressors of Build 2 with those of Build 1 shows different efficiency levels, particularly at low speeds. This difference is a consequence of measurement of the interstage temperature by two resistance temperature detectors at the first-stage diffuser exit, where flow mixing has not been completed.

Build 2 testing essentially confirmed the projected pressure ratio levels that were anticipated in TR 73-4 with unmodified components at 100 and 103 percent design speed, with peak overall efficiencies up to 1 percentage point lower as a consequence of operating with finite clearance gaps.

Build 3/4

Analysis of the performance data from Build 2 showed that the first-stage impeller was approaching choke at design speed. Thus, to delay choke, the first stage was rematched for Build 3 by decreasing the diffuser throat area 3-1/2 percent. This was effected by reducing first-stage diffuser vane height from 0.280 to 0.270 inch. Additionally, the cutback on the intermediate inducer blades was modified as shown in Figure 15 to provide a small increase in effective inducer throat area.

The cold axial clearances for the first- and second-stage impellers were set at 0.035 inch and 0.027 inch, and the inlet proximity probe (Figure 3) was used to monitor shaft axial displacement relative to the casing at each test condition.

Compressor performance evaluation was conducted with zero first-stage bleed at 60, 70, and 80 percent speed, after which proximity probe data indicated the possibility of rubbing at 90 percent speed. The first-stage cold axial clearance was therefore increased to 0.058 inch, by reshimming, and performance evaluation completed at 90, 95, and 100 percent speed. During surge at 100 percent speed, a rig overspeed shutdown was experienced, with resulting rapid deceleration of the rig. The rig was subsequently brought back to 80 percent speed, where performance checks revealed data repeatability, but the rig rotor vibration level was unacceptable. Stripdown of he rig revealed that the overspeed condition had relaxed the drive-turbine interference fit to the shaft, causing loss of pilot and balance. The rotating assembly was rebalanced and the rig assembled for Build 4 with first- and second-stage impeller cold clearances of 0.047 and 0.027 inch respectively. Repeat testing was conducted at 100 percent design speed with zero first-stage bleed followed by testing at 100, 95, and 90 percent speed with 1-1/2 percent bleed. The first stage was then reshimmed to a cold axial clearance of 0.036 inch, and testing continued at 80, 70, and 60 percent design speed with 1-1/2 percent bleed. Supplementary low-speed data at 40 and 20 percent were recorded with zero first-stage bleed.
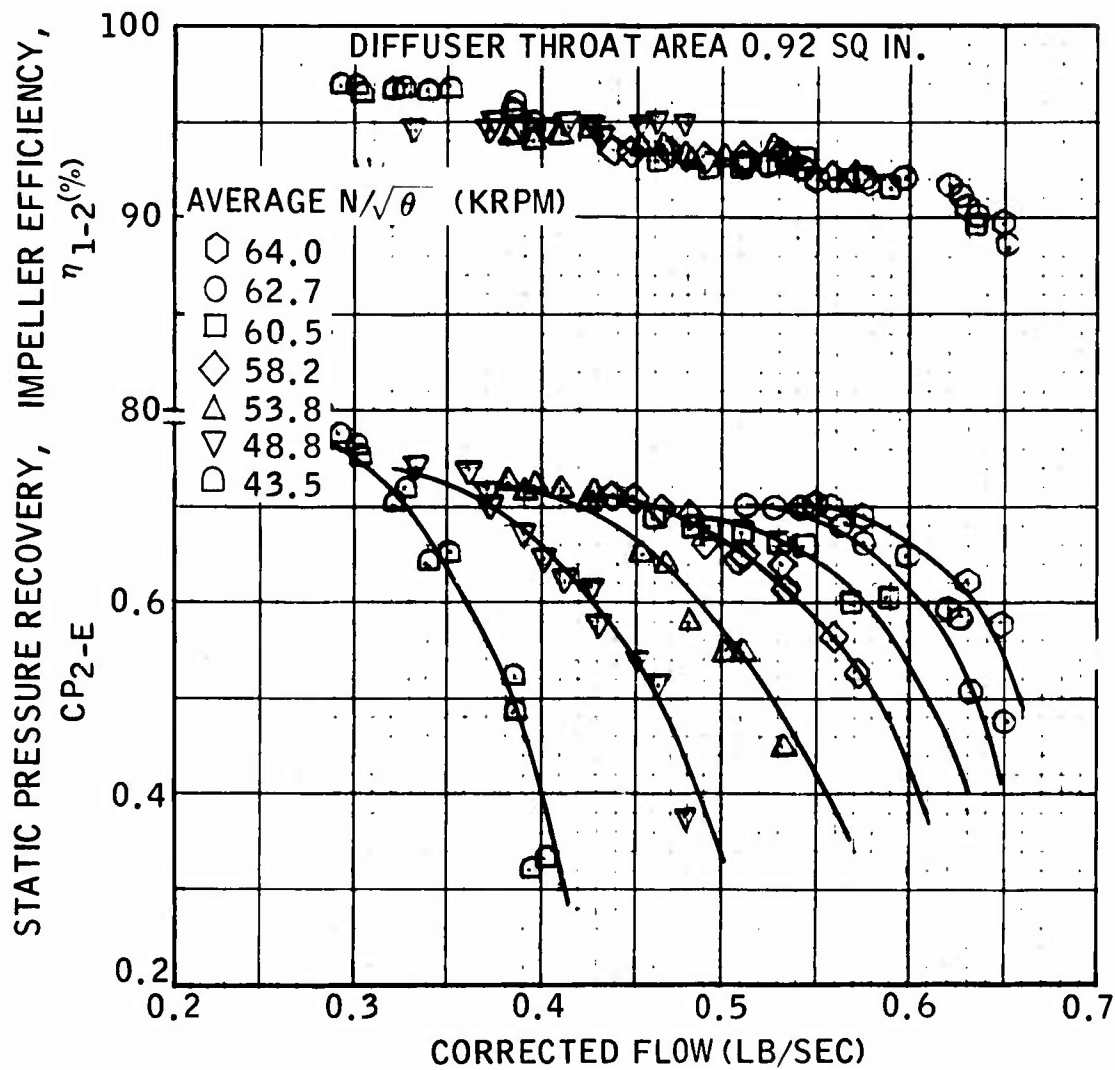
18

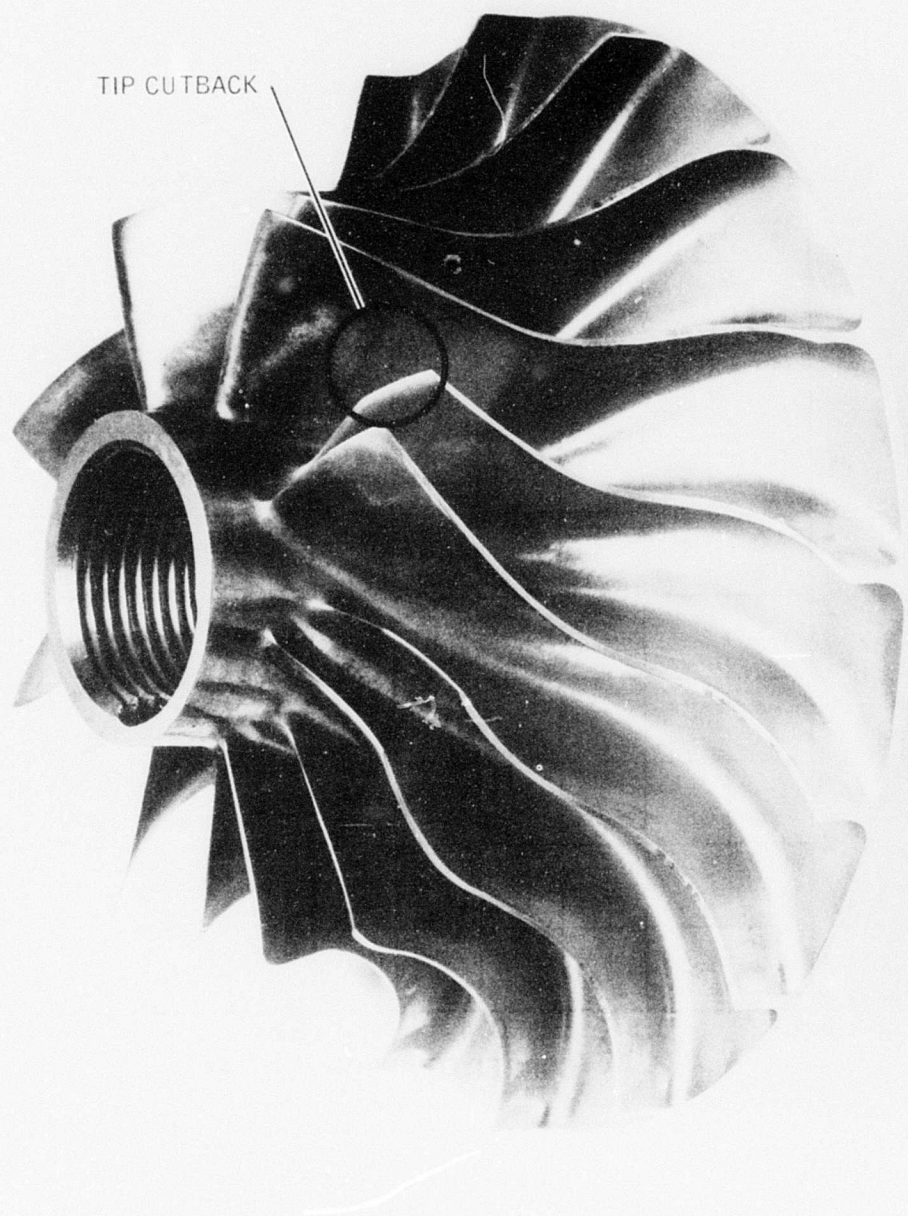Figure 14. Second-Stage Impeller and Diffuser Matching, Build 2.

TIP CUTBACK

Figure 15.   First-Stage Inducer Modification, Build 3/4.

20

Build 3/4 Overall Performance

The corrected overall compressor performance, measured with zero and 1-1/2 percent first-stage diffuser throat bleed, is shown in Figures 16 and 17. Peak overall efficiency at 100 percent design speed with zero bleed and an average first-stage axial clearance of 0.017 inch was 78 percent at a pressure ratio of 13.2 and an airflow of 1.94 pps, compared with design estimates of 79 percent at a pressure ratio of 14.0 and an airflow of 2.0 pps. Peak overall efficiency with 1-1/2 percent bleed was essentially the same as with zero bleed. First-stage bleed did improve the low-speed surge; however, since the compressor exhibits an extremely wide flow range with zero bleed, the use of first-stage diffuser bleed is not warranted.

Hot first-stage axial clearances, as determined from cold setting and proximity probe data, are shown for each test speed on Figures 16 and 17. Second-stage hot axial clearance at 100 percent speed was estimated to be on the order of 0.015 inch. Rematching the first-stage compressor improved the high-speed performance, as anticipated, without a reduction in maximum (choke) flows. Compared with Build 2, the surge pressure ratio at 100 percent speed and zero bleed increased from 12.9 to 13.7 and peak efficiency increased 1 percentage point. Performance data were recorded at 40 and 20 percent with zero bleed, without changing the instrumentation, to more accurately cover the lower levels of pressures and temperatures; thus the low-speed efficiencies shown on Figure 16 are subject to an increased degree of uncertainty.

Build 3/4 Stage Performance

Test performance of the first stage with zero bleed is shown on Figure 18. Peak first-stage efficiency and pressure ratio at 100 percent design speed increased from 77 percent and 4.7 on Build 2 to 78 percent and 4.9, compared with design values of 81 percent and 4.9. Note that assessment of first-stage efficiency is dependent upon the accuracy of the interstage temperature measurement, which was known to be erratic at lower speeds. As a result, individual stage efficiency data at 40 and 20 percent design speed are not plotted on Figure 18. Further reduction in first-stage clearance and operation with ambient pressure suction would assist in raising first-stage efficiency closer to the design value. First-stage inlet pressure at 100 percent speed was 11.0 psia. Rematching of the first stage achieved the required results, in that pressure ratio and efficiency increased without any reduction in flow range. Impeller and diffuser matching of the first stage is shown on Figure 19.

Test performance of the second-stage compressor is shown on Figure 20 at the various average test-corrected speeds, based upon second-stage inlet temperature. At 100 percent design speed, peak efficiency was 85 percent (based upon $\gamma = 1.395$) with a pressure ratio of 2.69 compared with design values of 83 percent and 2.86. As discussed in TR 73-4, the major reason for decreased pressure ratio is a lower compressor work factor (0.717) compared with the design value of 0.758. Design second-stage inlet prewhirl was 7 degrees in the direction of rotation. A test prewhirl on the order of 20 degrees would result in the reduced work factor. Relative matching of the second-stage impeller and its vaned diffuser is shown in Figure 21.
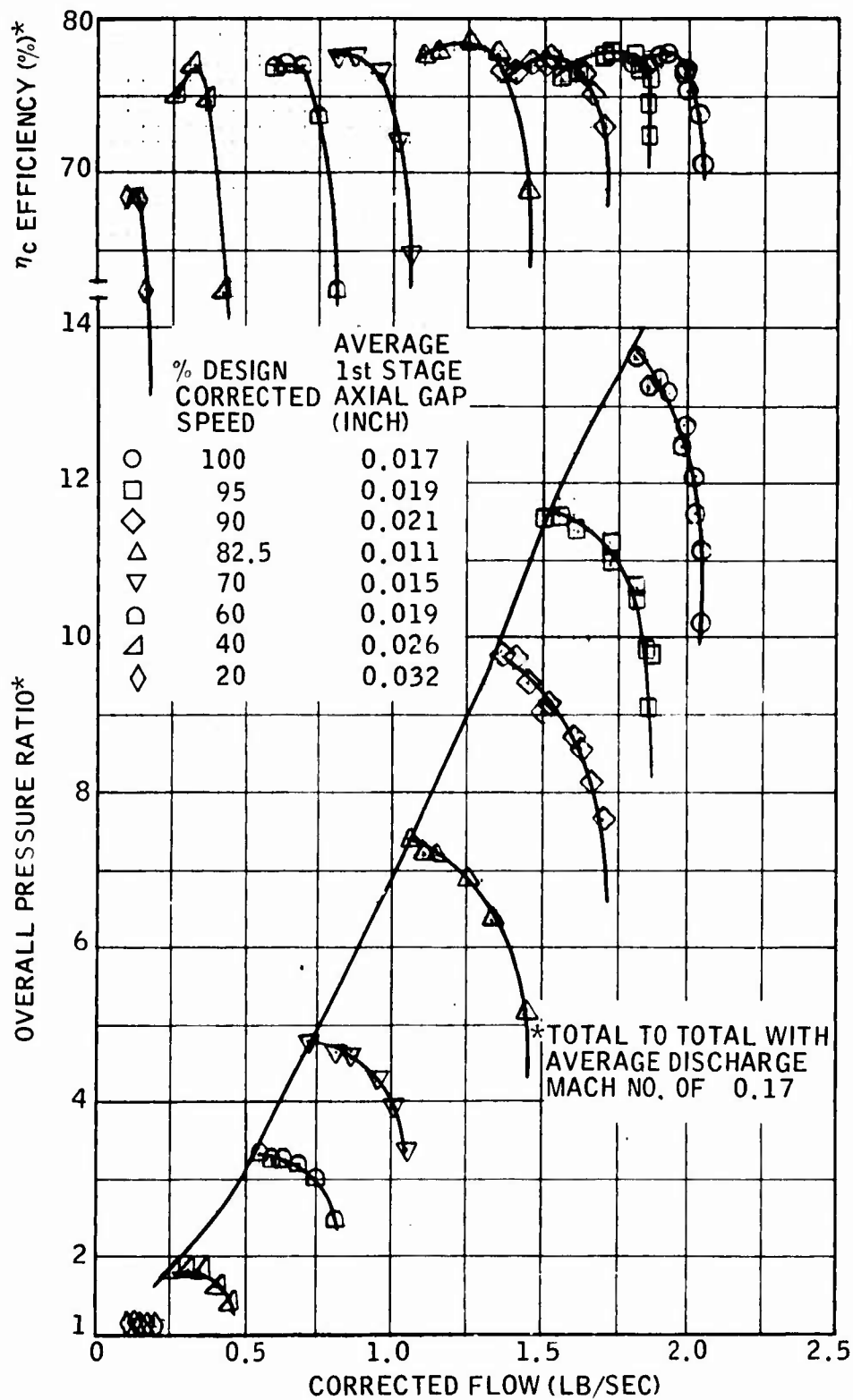
Figure 16. Overall Compressor Performance, Build 3/4 (Zero Bleed).
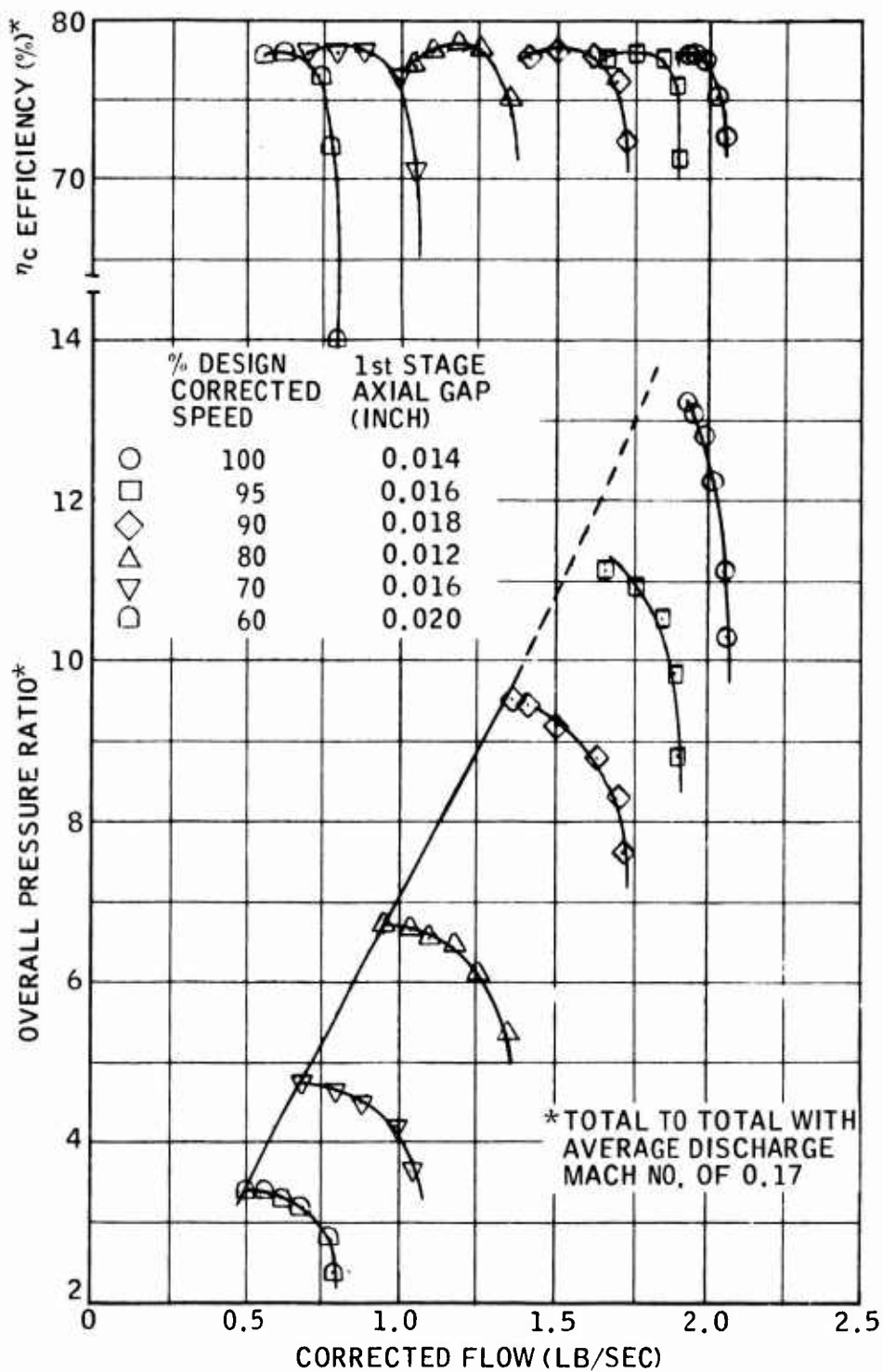
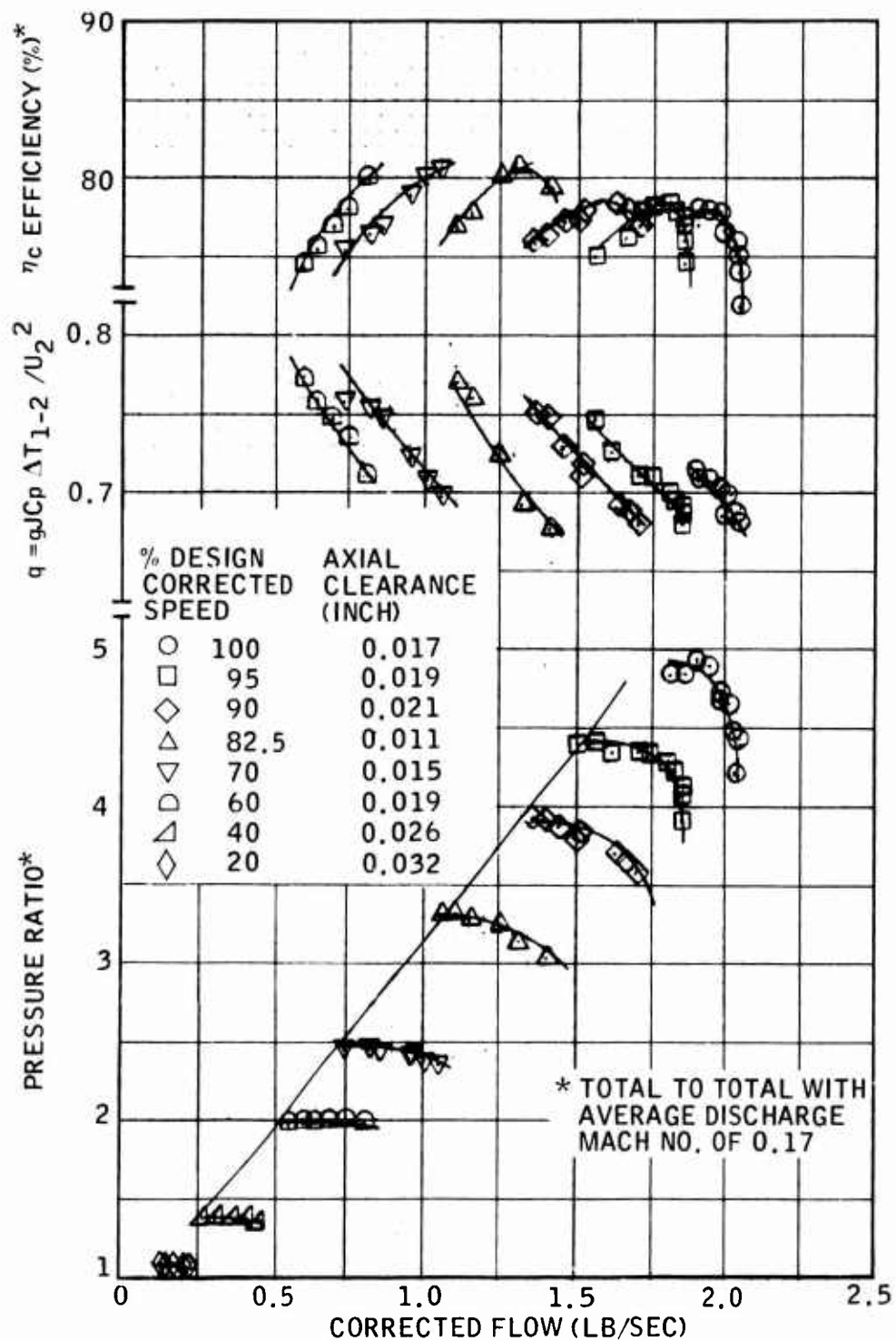Figure 17. Overall Compressor Performance, Build 3/4 (1-1/2 Percent Bleed).

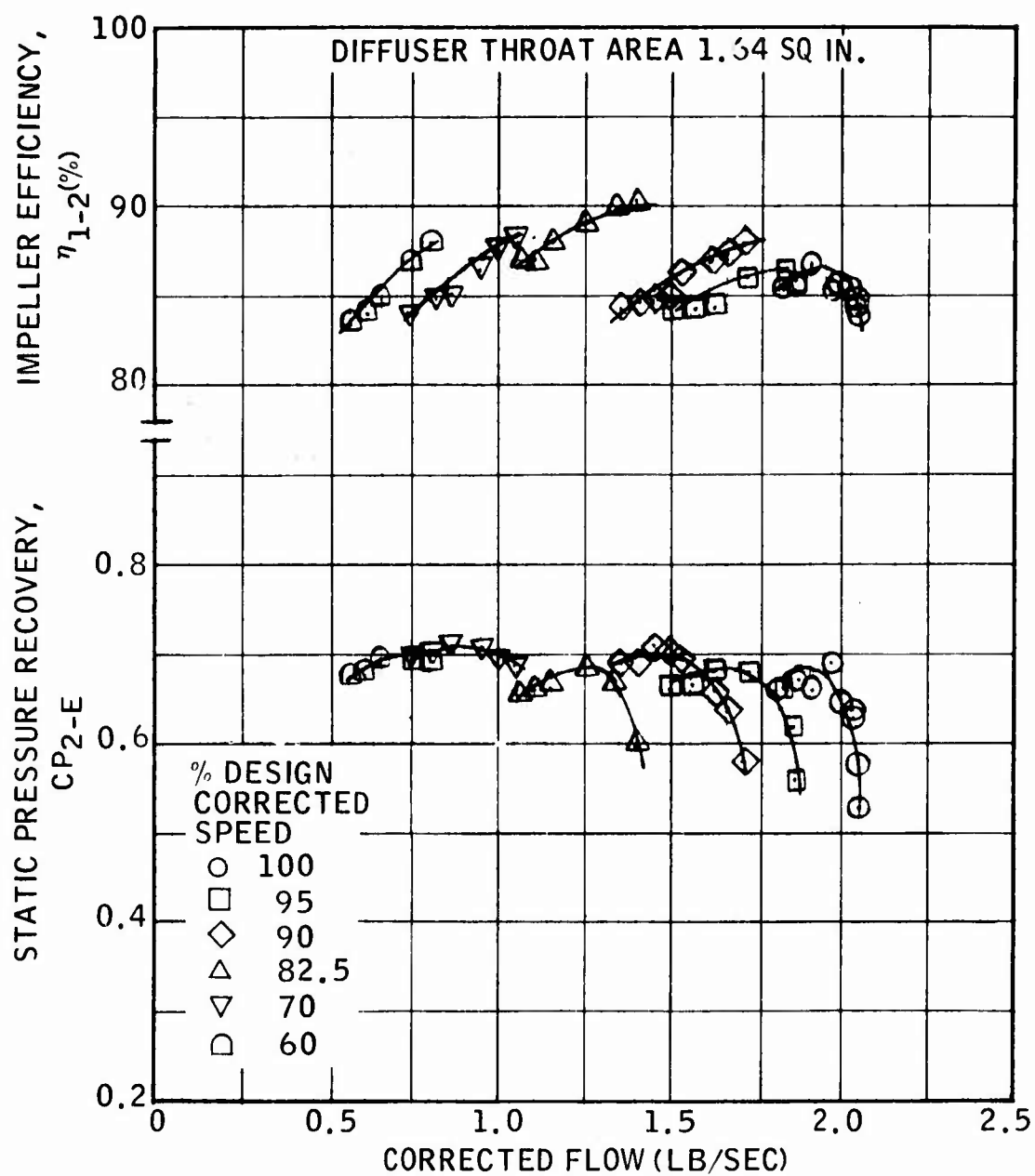Figure 18. First-Stage Performance, Build 3/4 (Zero Bleed).

Figure 19.   First-Stage Impeller and Diffuser Matching, Build 3/4 (Zero Bleed).
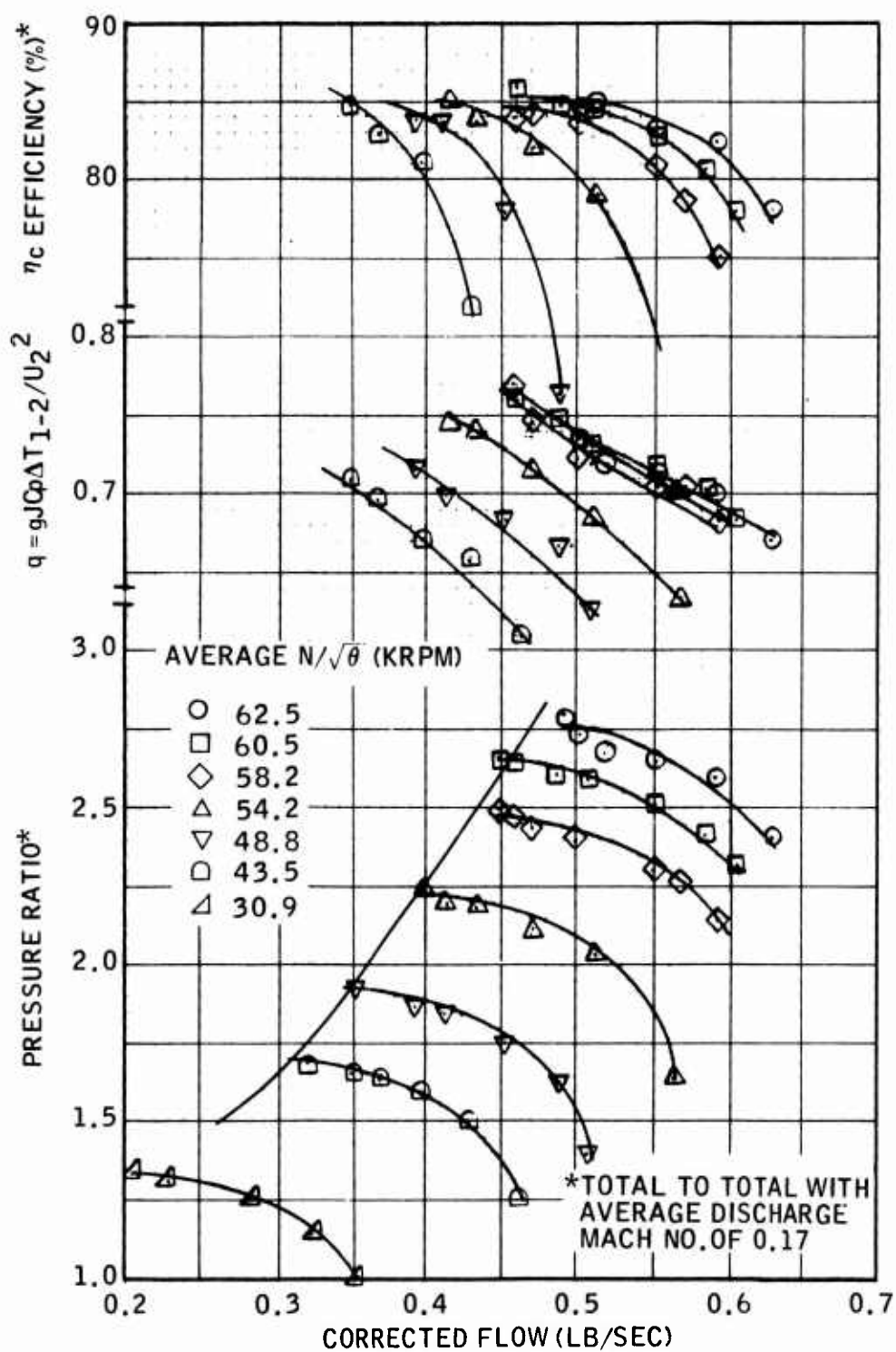
25

Figure 20. Second-Stage Performance, Build 3/4.
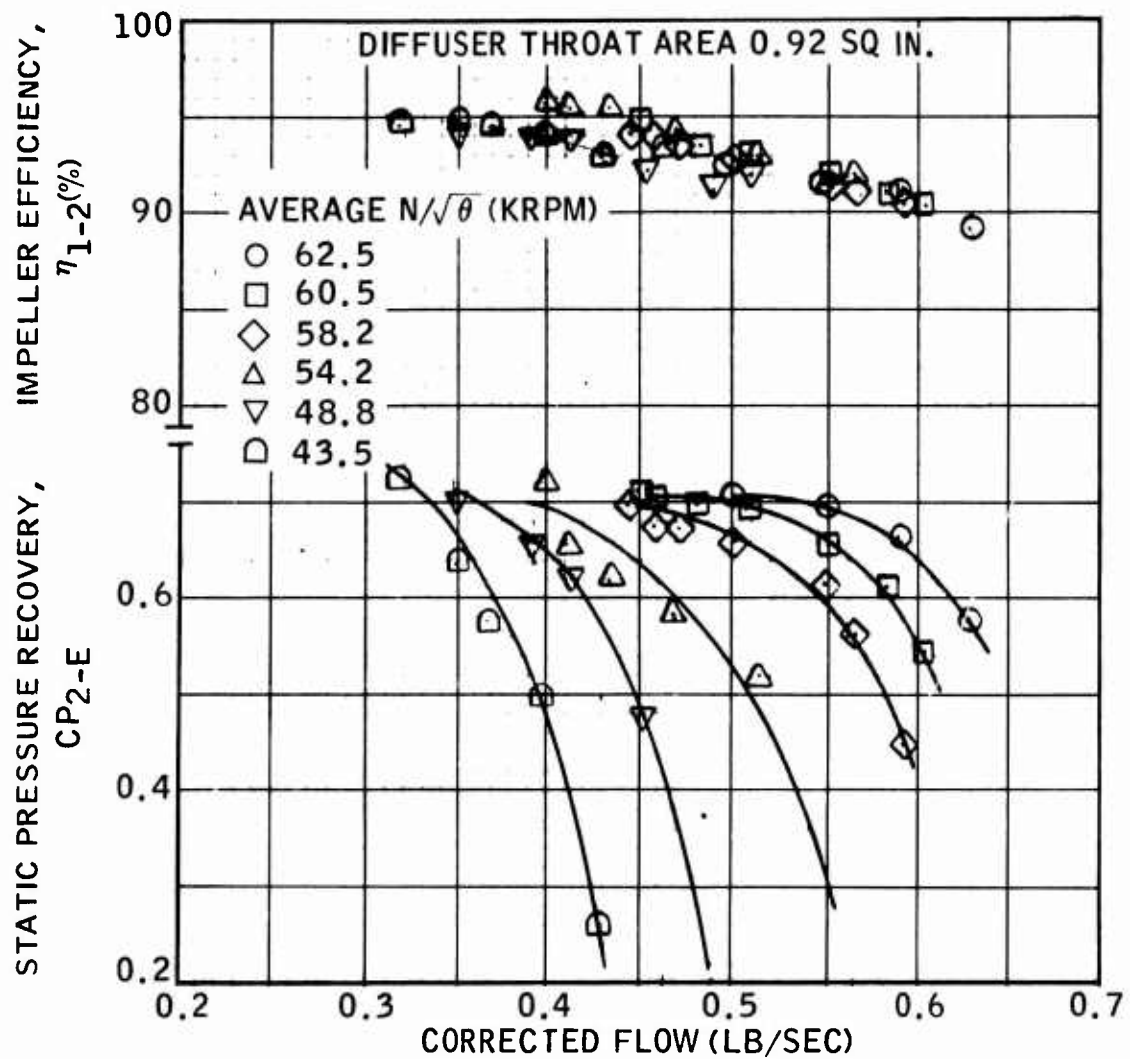
Figure 21. Second-Stage Impeller and Diffuser Matching, Build 3/4.

Compressor Surge

The compressor surge line was determined by gradually closing the single discharge butterfly valve until audible surge (compressor stall) was observed at the test speeds. At speeds up to 90 percent design speed, the surges were quite mild, severity and noise increasing with higher speeds. No audible surges were experienced at 20 and 40 percent design speed; the minimum flow points shown on Figure 16 are the points at which compressor discharge pressure no longer increased.

The shape of the surge line is quite smooth, without any knees (or kinks), and provides ideal matching for gas turbine application.

PERFORMANCE SUMMARY

Analysis of the overall and stage test performances of the subject two-stage centrifugal compressor showed the corrected performances to be as shown in the table for both a constant and variable specific heat analysis. The apparent low and high test efficiencies of the first and second stages cast doubt upon accuracy in measurement of the interstage temperature, and a more realistic split may well be 79 percent for the first stage and 84 percent for the second stage. Overall efficiency, based upon variable specific heat analysis, is 76.6 percent--still relatively high for a compressor of this size and pressure ratio capability. To illustrate the suitability of this compressor design for gas turbine application, a turboshaft matching exercise was completed, the results of which are shown on Figure 22 (based upon Build 3/4, zero bleed compressor test data). The equilibrium operating line was selected to pass through a pressure ratio of 13.2 at 100 percent design speed, and follows the island of peak compressor efficiency over the complete compressor map. Surge margin from the equilibrium operating line is extensive and should allow a simple form of turboshaft fuel control system.
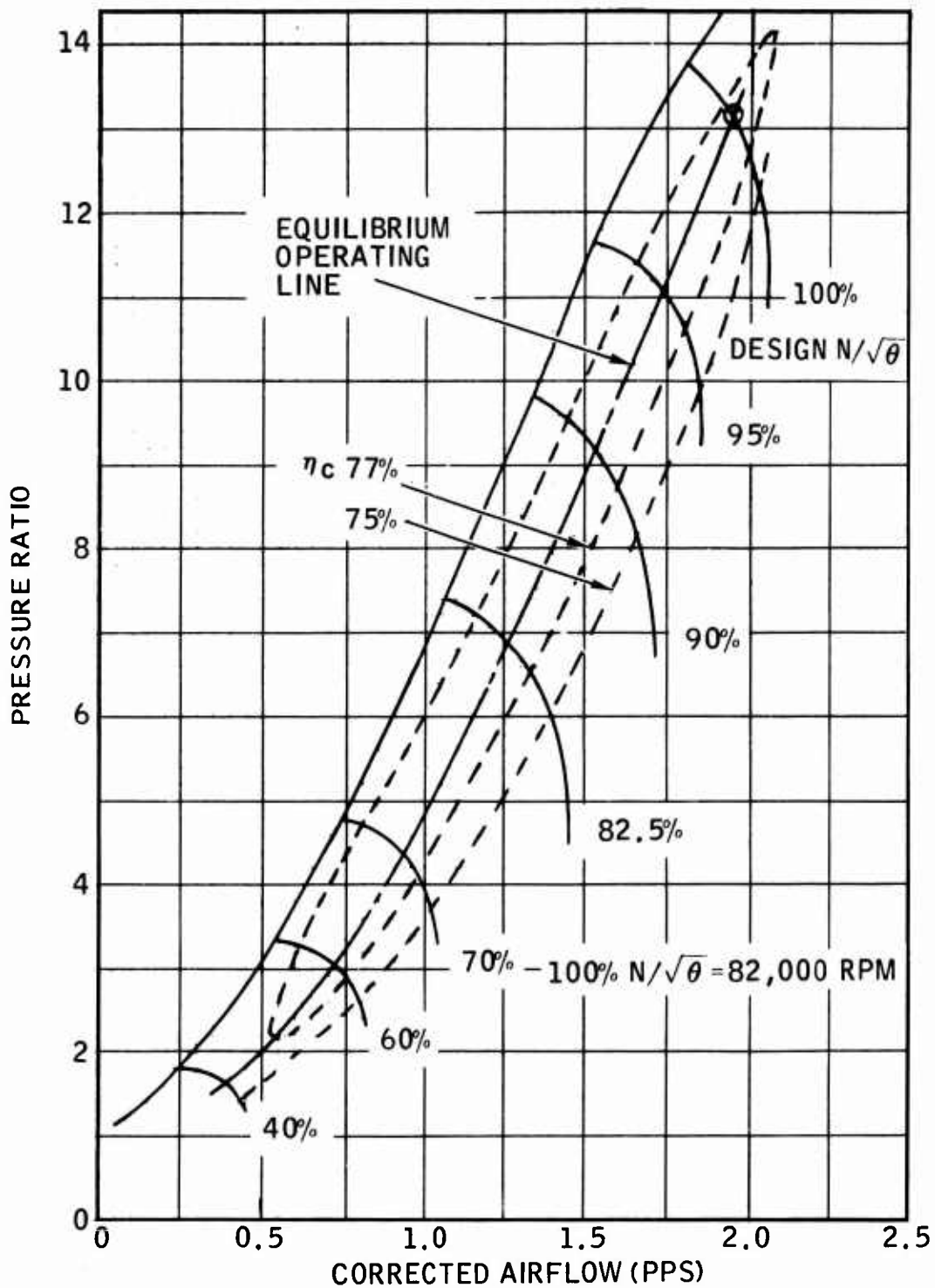
Figure 22. Typical Turboshaft Operating Line (Free Power Turbine).

COMPRESSOR CORRECTED PERFORMANCE COMPARISONS

ITEM	CASE *		
	1	2	3
Rotational Speed, krpm	82	82	82
Inlet Pressure, psia	14.7	11.0	11.0
Inlet Temperature, °F	60	60	60
Inlet Airflow, pps	2.05	1.94	1.94
First-Stage Pressure Ratio	4.9	4.9	4.9
First-Stage Efficiency, %	81	78	78.2
Second-Stage Pressure Ratio	2.86	2.69	2.69
Second-Stage Efficiency, %	83.6	85	82.0
Overall Pressure Ratio	14.0	13.2	13.2
Overall Efficiency, %	79.0	78	76.6

* Case

    1.   Original Design   ($\gamma = 1.395$)

    2.   Test data, Build 3/4   ($\gamma = 1.395$)

    3.   Test data, Build 3/4   (Variable Specific Heat)

Note: All efficiencies based upon discharge total pressure with average stage exit Mach numbers of 0.17.

CONCLUSIONS

Extensive performance data were obtained for the subject two-stage centrifugal compressor for two basic aerodynamic configurations with zero and 1-1/2 percent first-stage diffuser throat bleed.

The second aerodynamic configuration, incorporating a minor rematch to the first-stage compressor, with zero bleed and 100 percent design speed (82,000 rpm), gave a peak overall compressor efficiency of 78 percent at a pressure ratio of 13.2 and an airflow of 1.94 pps.

The compressor exhibited extremely wide flow ranges between surge and choke, with zero first-stage diffuser bleed. Use of 1-1/2 percent diffuser bleed provided a minor improvement in the low speed surge line.

RECOMMENDATIONS

Successful development of the subject two-stage centrifugal compressor has demonstrated that high pressure ratios with acceptable efficiencies can be obtained without the requirements for variable geometry or interstage bleed. The basic simplicity of the two-stage centrifugal compressor thus lends itself to application in small, low-cost gas turbines requiring simple, inexpensive control systems, unrestrained by surge margin considerations and capable of increased foreign object damage protection.

The results of this program warrant technological effort equivalent to that which has, in the past, been devoted to axial-centrifugal compressor configurations.

Continued development of the two-stage centrifugal compressor is therefore recommended to obtain even higher pressure ratios and efficiencies for use in advanced small gas turbine engines.

LIST OF SYMBOLS

Cp	Specific heat at constant pressure, 0.243 Btu/lb°R for air
CP	Diffuser static pressure recovery = $\dfrac{\text{Static pressure rise}}{\text{Inlet dynamic head}}$
g	Gravitational constant, 32.2 ft/sec^2
J	Joules equivalent of heat, 778 ft-lb/Btu
N	Rotational speed, rpm
KRPM	Rotational speed, thousands of rpm
q	Work factor, $\dfrac{gJC_p\Delta T}{U_2{}^2}$
T	Temperature, °F, °R, or stagnation flow conditions
U	Blade tip speed, ft/sec
W	Airflow, lb/sec
γ	Specific heat ratio, 1.395
Δ	Difference
η	Efficiency, based on temperature rise
θ	$\dfrac{\text{Inlet temperature, °R}}{519}$

SUBSCRIPTS

1	Impeller inlet
2	Impeller tip
E	Exit